



Springer

Dear Author:

Please find attached the final pdf file of your contribution, which can be viewed using the Acrobat Reader, version 3.0 or higher. We would kindly like to draw your attention to the fact that copyright law is also valid for electronic products. This means especially that:

- You may not alter the pdf file, as changes to the published contribution are prohibited by copyright law.
- You may print the file and distribute it amongst your colleagues in the scientific community for scientific and/or personal use.
- You may make an article published by Springer-Verlag available on your personal home page provided the source of the published article is cited and Springer-Verlag is mentioned as copyright holder. You are requested to create a link to the published article in LINK, Springer's internet service. The link must be accompanied by the following text: The original publication is available on LINK **<http://link.springer.de>**. Please use the appropriate URL and/or DOI for the article in LINK. Articles disseminated via LINK are indexed, abstracted and referenced by many abstracting and information services, bibliographic networks, subscription agencies, library networks and consortia.
- You are not allowed to make the pdf file accessible to the general public, e.g. your institute/your company is not allowed to place this file on its homepage.
- Please address any queries to the production editor of the journal in question, giving your name, the journal title, volume and first page number.

Yours sincerely,

Springer-Verlag Berlin Heidelberg

Carsten Krebs · J. Martin Bollinger Jr.
Elizabeth C. Theil · Boi Hanh Huynh

Exchange coupling constant J of peroxodiferric reaction intermediates determined by Mössbauer spectroscopy

Received: 23 January 2002 / Accepted: 25 March 2002 / Published online: 27 April 2002
© SBIC 2002

Abstract Oxygen activation at a carboxylate-bridged diiron cluster is employed by a number of enzymes for diverse biological functions. The mechanisms by which O_2 is activated at the diferrous clusters have been studied in detail and peroxodiferric reaction intermediates have been observed in several of these diiron proteins. To understand further the magnetic properties of this common reaction intermediate, we have used Mössbauer spectroscopy to determine the magnitude and sign of the exchange coupling constant J (in the exchange Hamiltonian $J S_1 \cdot S_2$) of the peroxodiferric intermediates generated during the reactions of O_2 with two different proteins, the recombinant M ferritin from frog and the site-directed variant W48F/D84E of the R2 subunit of ribonucleotide reductase from *Escherichia coli*. Both intermediates are antiferromagnetically coupled with a moderate coupling constant J of $50 \pm 10 \text{ cm}^{-1}$ for R2-W48F/D84E and $75 \pm 10 \text{ cm}^{-1}$ for M ferritin. This work demonstrates the capability of Mössbauer spectroscopy to determine exchange coupling constants of diiron complexes, including reaction intermediates. The approach and its limitations are described.

Keywords Peroxodiferric complex · Exchange coupling constant · Oxygen activation · Reaction intermediate · Mössbauer measurement

Introduction

Proteins containing carboxylate-bridged diiron clusters form a class of enzymes that utilize molecular oxygen for diverse, chemically difficult transformations. Examples include the hydroxylase component (MMOH) of the soluble methane monooxygenase system [1, 2], which effects the hydroxylation of methane to methanol, the stearyl-acyl carrier protein Δ^9 -desaturase ($\Delta 9D$) [3], which introduces a *cis* double bond between carbons 9 and 10 of stearyl-ACP, protein R2 of class I ribonucleotide reductase [4], which oxidizes a tyrosine residue to the corresponding tyrosyl radical, and ferritin, which uses O_2 to rapidly oxidize Fe^{2+} to Fe^{3+} at the diiron site during the initial stages of iron deposition [5, 6]. Stopped-flow absorption [7] and rapid freeze-quench Mössbauer [8, 9] studies have shown that the diferrous form of MMOH reacts with O_2 to form a peroxodiferric intermediate (H_{peroxo} or P) that exhibits a broad absorption band at 725 nm and a unique Mössbauer spectrum (a single quadrupole doublet with $\Delta E_Q = 1.51 \text{ mm/s}$ and $\delta = 0.66 \text{ mm/s}$, indicating a similar coordination environment for the two ferric sites). Reaction of O_2 with the fully reduced $\Delta 9D$ in the presence of stearyl-ACP also yields a peroxodiferric complex with similar optical absorption ($\lambda_{\text{max}} = 700 \text{ nm}$) [10] but a distinct Mössbauer spectrum (two quadrupole doublets with ΔE_Q values of 1.06 and 1.90 mm/s and δ values of 0.64 and 0.68 mm/s, respectively, indicating different coordination environments for the two ferric sites) [11]. Resonance Raman investigations showed a μ -1,2-peroxide binding mode for this $\Delta 9D$ reaction intermediate, which is relatively stable at room temperature (half-life $\sim 30 \text{ min}$) and decays by an oxidase reaction without forming the desaturated product [10]. For the R2 protein, a peroxodiferric intermediate has not been detected in the wild-type R2. However, in the site-directed variants R2-D84E and R2-W48F/D84E, in which an aspartate ligand (D84) has been substituted by a glutamate to

C. Krebs · B.H. Huynh (✉)
Department of Physics, Emory University,
Atlanta, GA 30322, USA
E-mail: vhuynh@emory.edu
Fax: +1-404-7270873

J.M. Bollinger Jr.
Department of Biochemistry and Molecular Biology,
Pennsylvania State University,
University Park, PA 16802, USA

E.C. Theil
CHORI (Children's Hospital Oakland Research Institute),
5700 Martin Luther King Jr. Way, Oakland,
CA 94609, USA

imitate the corresponding Fe site in MMOH, peroxodiferric species ($R2_{\text{peroxo}}$) exhibiting spectroscopic properties similar to those of H_{peroxo} have been observed during oxygen activation [12, 13]. Resonance Raman studies of the relatively stable $R2_{\text{peroxo}}$ (half-life 2–3 s) in R2-W48A/D84E also indicate a μ -1,2-binding mode for the peroxide ligand [14]. Although the geometrical structure of $R2_{\text{peroxo}}$ is not known, its spectroscopic features are closely matched by those of a structurally determined peroxodiferric model complex [15], which shows a $\text{Fe}_2(\mu$ -1,2-peroxo)(μ -1,3-benzoato) $_2$ core with a Fe-Fe separation of 4.0 Å. In the case of ferritin, a peroxodiferric intermediate (F_{peroxo}) was found to accumulate in H-type ferritins during the ferroxidase reaction (rapid oxidation of Fe^{2+} by ferritin using O_2 as an oxidant) [6, 16, 17]. Detailed spectroscopic studies showed that F_{peroxo} is spectroscopically and structurally distinct from the peroxodiferric intermediates mentioned above. It exhibits a broad absorption band at 650 nm and a single Mössbauer quadrupole doublet having $\Delta E_Q = 1.06$ mm/s and $\delta = 0.62$ mm/s [6, 17]. Although rapid freeze-quench resonance Raman investigations of F_{peroxo} showed a μ -1,2-binding mode for the peroxide ligand [18], similar to that of other peroxodiferric intermediates, the Fe-Fe distance was found by EXAFS measurements to be unusually short (2.53 Å) [19]. This structural difference between F_{peroxo} and other protein peroxodiferric intermediates has been suggested to reflect different geometrical arrangements of amino acid residues of the diiron sites as the means for the protein to control the fates of the intermediates [19]. In the O_2 -activating enzymes, such as R2 and MMOH, the peroxodiferric intermediates decay to potent oxidants that oxidize organic substrates and form the diferric products, while in ferritin, the decay of the peroxodiferric intermediate produces μ -oxo and/or μ -hydroxo diferric biomineral precursors with the release of hydrogen peroxide.

To gain insights into the electronic structures of these peroxodiferric intermediates detected in the diiron proteins, we have used Mössbauer spectroscopy to determine the exchange coupling constant J (as defined in the exchange Hamiltonian $J\mathbf{S}_1\cdot\mathbf{S}_2$) of $R2_{\text{peroxo}}$ and F_{peroxo} . Methods usually employed for the determination of J are saturation magnetization measurements and temperature-dependent ^1H NMR spectroscopy. Both techniques are, however, difficult, if not impossible, to apply to transient reaction intermediates. High-temperature high-field Mössbauer spectroscopy can be used to determine J of coupled Fe species and has been applied to a bis- μ -oxo diferric model compound [20, 21]. In this study we show that, in contrast to the other methods (magnetization and ^1H NMR), the Mössbauer approach can also be used to determine the exchange coupling constants of diiron reaction intermediates, such as $R2_{\text{peroxo}}$ and F_{peroxo} , trapped by the rapid freeze-quench technique.

Materials and methods

General

The samples were prepared according to procedures described in the literature [6, 13]. The Mössbauer spectra were recorded in spectrometers that operate in a constant acceleration mode in a transmission geometry and that have been described elsewhere [5]. The zero velocity of the spectra refers to the centroid of a room-temperature spectrum of a metallic iron foil. Spectral simulations were performed using the program WMOSS (WEB Research).

Determination of J of diiron complexes using Mössbauer spectroscopy

Mössbauer spectroscopy can be used to determine the exchange coupling constant J of Fe-containing metal clusters. It is particularly sensitive to systems having a diamagnetic ground state and excited paramagnetic states accessible at temperatures where Mössbauer spectroscopy is applicable (below 240 K), such as an antiferromagnetically coupled diferric compound [20, 21]. In the following sections, the general strategy for determining J of an antiferromagnetically coupled diferric compound by Mössbauer spectroscopy is described.

The first step involves analysis of spectra recorded at 4.2 K, where the ground state is almost exclusively populated. From the zero-field spectrum, the isomer shift δ and the quadrupole splitting parameter ΔE_Q are obtained. From the spectra recorded in strong applied fields, the asymmetry parameter η can be determined and the diamagnetism of the ground state can be established. Small internal magnetic fields have been observed for the ground states of two antiferromagnetically coupled diferric species: the diiron cluster of oxidized MMOH from *Methylosinus trichosporium* OB3b and a model compound [22]. This occurrence has been ascribed to the presence of an antisymmetric exchange interaction [22]. It is therefore important to ascertain the diamagnetism of the ground state of the species under investigation. The second step involves analysis of spectra recorded at elevated temperatures, which should be sufficiently high for the excited electronic states to be populated. As the excited states are paramagnetic, population of the excited states may induce an internal field at the Fe nucleus, of which the magnitude and sign can be determined by analyzing the high-temperature Mössbauer spectra. Since the internal field is a function of the exchange coupling constant J , temperature T , and applied magnetic field \mathbf{B} (see below), comparison of the experimentally determined internal field with theoretical values would then allow for an estimation of J (both T and \mathbf{B} are known experimentally). Obviously, this approach requires a good theoretical model for the system under investigation and is most useful in the region where the internal field is sensitive to the variation of J .

In our analysis, we have assumed that at high temperatures (above 77 K) the fluctuation rate between the electronic states of the peroxodiferric intermediates is fast compared to the Larmor frequency of the ^{57}Fe nuclei. This assumption holds for most Fe clusters in proteins and model complexes. With this assumption, the internal field at the Fe nucleus can be calculated as:

$$\mathbf{B}_{\text{int}} = \langle S \rangle_{\text{av}} \cdot \mathbf{A} / g_n \beta_n \quad (1)$$

where \mathbf{A} is the magnetic hyperfine coupling tensor and $\langle S \rangle_{\text{av}}$ is the thermal average of the expectation value of the total spin S , which can be calculated as the sum of the spin expectation values, $\langle S \rangle_i$, of all the electronic states, i , weighted by their Boltzmann population factors:

$$\langle S \rangle_{\text{av}} = \frac{\sum \langle S \rangle_i \exp(-E_i/kT)}{\sum \exp(-E_i/kT)} \quad (2)$$

In Eq. 2, E_i represents the energy of the i th electronic state. Both E_i and $\langle S \rangle_i$ are calculated by using the following spin Hamiltonian describing the electronic states of an exchange coupled diferric system:

$$\mathbf{H} = J \mathbf{S}_1 \cdot \mathbf{S}_2 + g\beta \mathbf{S} \cdot \mathbf{B} \quad (3)$$

Here, $S_1 = S_2 = 5/2$ are the intrinsic spins of the two high-spin ferric ions and $\mathbf{S} = \mathbf{S}_1 + \mathbf{S}_2$ is the system spin. The first term describes the exchange interaction between these two Fe sites and the second term describes the Zeeman interaction between the system spin \mathbf{S} and the magnetic field \mathbf{B} . The zero-field interaction has been neglected since it is generally small for non-heme high-spin ferric species [20, 23]. Under these assumptions (i.e., a situation where Eq. 3 is valid), the system spin S and the magnetic quantum number M , representing the spin projection along the magnetic field \mathbf{B} , are good quantum numbers and can be used to describe the electronic states of the system. The energies and spin expectation values for the 36 coupled states can then be expressed, respectively, as:

$$E_{S,M} = \frac{1}{2}JS(S+1) + g\beta MB \quad (4)$$

and:

$$\langle S \rangle_{S,M} = M \quad (5)$$

It can be seen from Eq. 4 that for an antiferromagnetically coupled high-spin diferric complex ($J > 0$) the ground state is diamagnetic ($S=0$) and the first excited state is a triplet with $S=1$ and $M=-1, 0$, and 1 . In the absence of an applied field ($B=0$), this triplet state is degenerate (see Eq. 4). The Boltzmann populations for the $M=-1$ and 1 states are equal and thus the contributions of these two states to $\langle S \rangle_{av}$ cancel (see Eq. 2). This same argument applies to all higher spin states (i.e., $S=2, 3, 4$, and 5), and therefore, in zero field, $\langle S \rangle_{av}$ is zero, resulting in an internal field $B_{int}=0$. The Mössbauer spectrum is then a simple quadrupole doublet, allowing the determination of δ and ΔE_Q at this temperature. In the presence of an applied field, the degeneracy is lifted owing to the Zeeman interaction and the situation changed. The energies of states with negative M values are lowered, causing an increase in the populations of these states, whereas the energies of states with positive M values are raised, causing a decrease of their populations. The net result is a small negative $\langle S \rangle_{av}$, and thus, an internal field oriented antiparallel to the applied field.

In Eq. 1, the magnetic hyperfine tensor \mathbf{A} is assumed to be the same for all the states with different values of S . This assumption is valid for a homodinuclear system with $S_1 = S_2$, because for such a system the following relation holds for all spin states [23]:

$$\mathbf{A} = \mathbf{a}/2 \quad (6)$$

where \mathbf{a} is the intrinsic magnetic hyperfine tensor of the individual Fe site. Generally, for high-spin ferric systems, the intrinsic \mathbf{a} tensor is almost isotropic, with values ranging from $a/g_n\beta_n = -20$ to -22 T [24]. To demonstrate the dependence of B_{int} on J , Fig. 1 shows (thick solid line) the internal field as a function of the exchange coupling constant J calculated by using the following parameters: $T = 125$ K, $B = 8$ T, and $a/g_n\beta_n = -21$ T. For $J < 40$ cm^{-1} the slope of the curve is steep, allowing for a very accurate determination of J . For larger J values, the curve becomes flatter and determination of J is less certain. Also shown in Fig. 1 are the contributions of the various total spin states to the internal field: the contribution of the $S=1$ state corresponds to the section from the abscissa to the first dotted line, the contribution of the $S=2$ state corresponds to the section from the first to the second dotted line, etc. Shown in the inset of Fig. 1 are the Boltzmann populations for all spin states as a function of J , calculated for $T = 125$ K and $B = 8$ T. For small J , all states are sufficiently populated and (except for the $S=0$ state) contribute significantly to the internal field. As the J value increases, states with higher spin values become less populated and contribute less to the internal field. Nevertheless, contributions from higher spin states must be considered, even though their populations may be small. For example, for $J = 50$ cm^{-1} the

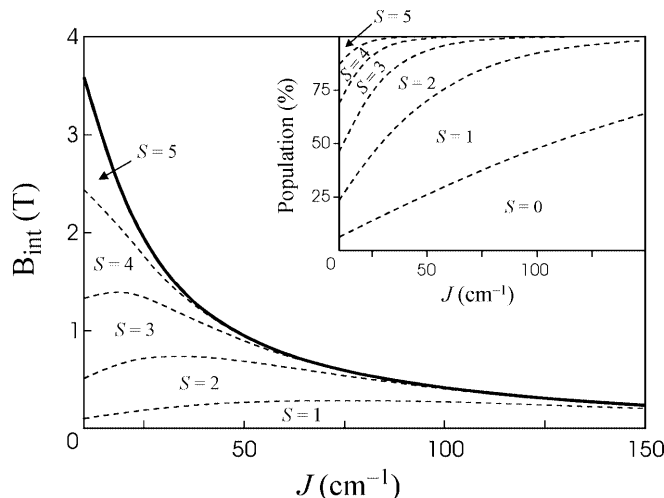


Fig. 1. Internal magnetic field at the Fe nuclei of a high-spin diferric system as a function of the exchange coupling constant J (solid line), calculated by using Eqs. 1, 2, 3, 4, 5 and the following parameters: temperature $T = 125$ K, external magnetic field $B = 8$ T, and magnetic hyperfine coupling constant $a/g_n\beta_n = -21$ T. Also shown are the individual contributions of the various spin states to the internal field. The contribution from the $S=1$ state is measured from the abscissa to the first dashed line, that from the $S=2$ state is measured from the first to the second dashed line, and that from the $S=3$ state is measured from the second to the third dashed line, etc. The inset shows the Boltzmann populations of the various spin states using the same representation

Boltzmann population of the $S=2$ state is only half of that of the $S=1$ state, yet its contribution to the internal field is twice of that of the $S=1$ state.

Results

Determination of J of F_{peroxo}

Using rapid freeze-quench Mössbauer spectroscopy, we have shown previously that in the reaction of frog M apoferritin with Fe^{2+} and O_2 , F_{peroxo} forms with a rate constant of ~ 80 s^{-1} and decays slowly with a rate of about $3\text{--}4$ s^{-1} (at 25 $^\circ\text{C}$), allowing a maximum accumulation of F_{peroxo} within $25\text{--}60$ ms of reaction time [6]. The Mössbauer investigation has also established that F_{peroxo} is an antiferromagnetically coupled diferric species with an $S=0$ ground state. For the current study, a sample was prepared (as described in [6]) by rapidly mixing M apoferritin with Fe^{2+} (36 Fe/ferritin 24-mer) and O_2 and freeze-quenching the reaction at 34 ms. The Mössbauer spectra of this sample are shown in Fig. 2. Spectrum A (hatched marks) was recorded at 125 K in the absence of an applied field and shows that 85% of the iron in the sample is in the form of F_{peroxo} , which exhibits a quadrupole doublet with parameters $\delta = 0.59 \pm 0.02$ mm/s and $\Delta E_Q = 1.01 \pm 0.03$ mm/s. A theoretical simulation of this doublet is plotted as a solid line in Fig. 2A. The observed parameters at 125 K are slightly smaller than the 4.2 K values of $\delta = 0.62$ mm/s and $\Delta E_Q = 1.06$ mm/s [6]. The reduction in isomer shift

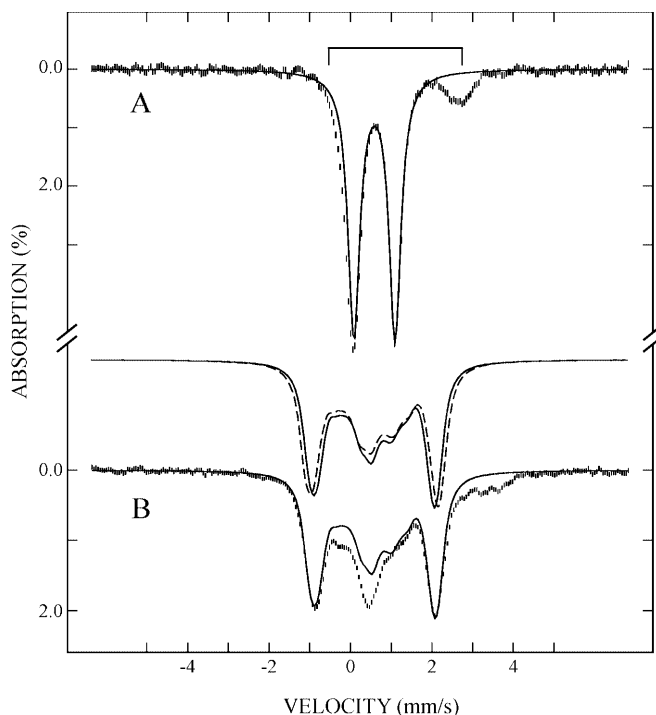


Fig. 2A, B. 125-K Mössbauer spectra of a freeze-quenched sample prepared by reacting apo M ferritin with Fe^{2+} (36 Fe/ferritin 24-mers) and O_2 for 34 ms at 25 °C. **A** The experimental spectrum (hatched marks) was recorded in zero field. The solid line is a theoretical simulation of F_{peroxo} using the parameters $\delta=0.59$ mm/s and $\Delta E_{\text{Q}}=1.01$ mm/s. The theoretical spectrum is scaled to 85% of the total Fe absorption. The bracket indicates the positions of the quadrupole doublet originating from the not-yet-reacted Fe^{2+} , which accounts for the remaining 15% Fe absorption. **B** The experimental data (hatched marks) was recorded in a field of 8 T applied parallel to the γ beam. The solid line overlaid with the experimental data is a theoretical simulation of F_{peroxo} using the parameters mentioned above and assuming an effective field of 7.4 T at the Fe nuclei. Plotted above the experimental data are theoretical spectra showing the influence of an internal magnetic field. The solid line is a simulation assuming an internal field of 0.6 T oriented antiparallel to the 8 T external field, and the dashed line is a simulation assuming a zero internal field.

is caused by the second-order Doppler shift and the observed slight decrease of ΔE_{Q} with increasing temperature is common for Fe proteins. Accounting for the remaining 15% of the Mössbauer absorption is a broad quadrupole doublet (indicated by a bracket; $\delta=1.25$ mm/s and $\Delta E_{\text{Q}}=3.55$ mm/s), which originates from the not-yet-reacted ferrous ions. To determine the internal field of F_{peroxo} at this temperature, a spectrum (Fig. 2B, hatched marks) of this same sample was recorded at 125 K in an external field of 8 T. The total magnetic splitting (separation between the two intense lines at -1 mm/s and $+2$ mm/s) of the spectrum depends on ΔE_{Q} and the effective field (external plus internal) at the Fe nuclei. Since ΔE_{Q} is known from the zero-field spectrum (Fig. 2A), the effective field can therefore be determined from the 8-T spectrum and was found to be 7.4 T. In other words, under the experimental conditions ($T=125$ K and $B=8$ T), F_{peroxo} has

an internal field of 0.6 T oriented antiparallel to the external field. The solid line overlaid with the experimental data is a theoretical simulation using the parameters mentioned above. The effect of the internal field on the spectrum is depicted by the two theoretical spectra plotted above the experimental data. The solid line is a spectrum corresponding to an internal field of 0.6 T, whereas the dashed line is a simulation without internal field. With the internal field known, we then used Fig. 1 to estimate the J value of F_{peroxo} and found that $J=75 \pm 10$ cm^{-1} . The uncertainty in J reflects both the variation of the intrinsic a value (20–22 T) and the uncertainty in our determination of the internal field.

The Boltzmann population factors for the spin states and the contribution of the respective spin state to $\langle S \rangle_{\text{av}}$ illustrate the necessity of including contributions from the less populated higher spin states for an accurate estimate of $\langle S \rangle_{\text{av}}$. With $J=75$ cm^{-1} and $T=125$ K, 47.2% of the molecules are in the first excited state, $S=1$, and they contribute 48.1% to $\langle S \rangle_{\text{av}}$. Only 13.9% of the molecules are in the $S=2$ state and yet they contribute 42.5% to $\langle S \rangle_{\text{av}}$. Significantly, 1.4% of the molecules that are in the $S=3$ state contribute 8.8% to $\langle S \rangle_{\text{av}}$ (see also Fig. 1).

Determination of J of $\text{R2}_{\text{peroxo}}$

For the determination of J of $\text{R2}_{\text{peroxo}}$, two samples were prepared: a $\text{R2}_{\text{peroxo}}$ sample in which apo R2-W48F/D84E was rapidly mixed with Fe^{2+} (3.4 Fe/R2) and O_2 at 5 °C and freeze-quenched at 440 ms reaction time, and a control sample in which the reaction was freeze-quenched at 25 ms. Previous kinetic investigations [13] have established that $\text{R2}_{\text{peroxo}}$ forms and decays with apparent first-order rate constants of 2.3 s^{-1} and 0.26 s^{-1} , respectively, and thus, at 440 ms reaction time, the major constituents in the reaction mixture are $\text{R2}_{\text{peroxo}}$ and the not-yet-reacted Fe^{2+} . Shown in Fig. 3A as hatched marks is the spectrum of the 440-ms sample recorded at 125 K in zero field. Two quadrupole doublets originating from $\text{R2}_{\text{peroxo}}$ and Fe^{2+} are observed. To deconvolute the spectrum and to remove the contributions from the Fe^{2+} species, we use the spectrum of the 25-ms sample, which contains mainly the not-yet-reacted Fe^{2+} . The solid line shown in Fig. 3A is the spectrum of the 25-ms sample recorded under identical conditions (125 K and zero field). To match the absorption intensities of the high-energy line of the Fe^{2+} quadrupole doublet at ~ 2.8 mm/s of the two samples, the spectrum of the 25-ms sample is scaled to 56% of the total intensity of the spectrum of the 440-ms sample, indicating that 56% of the Fe in the 440-ms sample has not yet reacted with O_2 . Removal of this Fe^{2+} contribution from the 440-ms sample spectrum resulted in the spectrum (hatched marks) shown in Fig. 3B. This spectrum represents the spectral contribution of $\text{R2}_{\text{peroxo}}$. It is a broad asymmetric quadrupole doublet that can be simulated by using two overlapping quadrupole

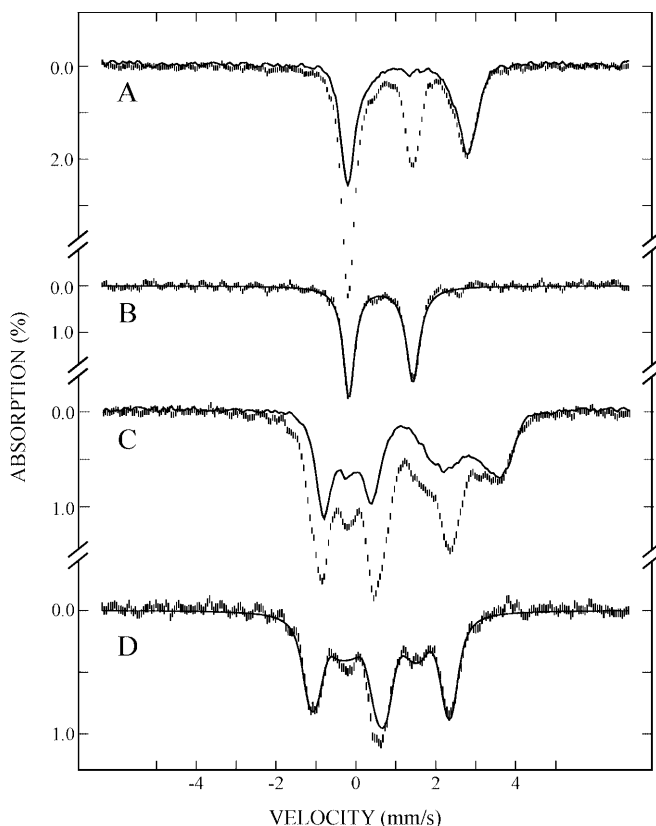


Fig. 3A–D. 125-K Mössbauer spectra of freeze-quenched samples prepared by reacting R2-W48F/D84E with Fe^{2+} (3.4 Fe/R2) and O_2 for 25 or 440 ms at 5 °C. **A** The *hatched-mark spectrum* is the experimental spectrum of the 440-ms sample recorded in zero field and the *solid line* is the zero-field spectrum of the 25-ms sample scaled to 56% of the total intensity of the spectrum of the 440-ms sample. **B** Removal of 56% of the 25-ms sample spectrum from the 440-ms sample spectrum (shown in **A**) results in the *hatched-mark spectrum*, which represents the zero-field spectrum of $\text{R2}_{\text{peroxo}}$. The *solid line* is a theoretical simulation of the $\text{R2}_{\text{peroxo}}$ spectrum using the parameters given in the text. **C** Experimental spectra of the 440-ms sample (*hatched marks*) and the 25-ms sample (*solid line*) recorded in a parallel field of 8 T. The *solid line spectrum* is scaled to 56% of the total intensity of the *hatched-mark spectrum*. **D** Removal of the contribution of the *solid-line spectrum* from the *hatched-mark spectrum* shown in **C** results in the 8-T spectrum of $\text{R2}_{\text{peroxo}}$ (*hatched marks*). The *solid line* is a theoretical simulation of the $\text{R2}_{\text{peroxo}}$ spectrum using the parameters given in the text

doublets of equal intensity and equal linewidth having the following parameters: $\delta(1) = 0.65$ mm/s, $\Delta E_{\text{Q}}(1) = 1.73$ mm/s, $\delta(2) = 0.61$ mm/s, and $\Delta E_{\text{Q}}(2) = 1.48$ mm/s. The solid line overlaid with the experimental data is the theoretical simulation using these parameters. To determine the internal field of $\text{R2}_{\text{peroxo}}$ at this temperature, we recorded a spectrum of the 440-ms sample at 125 K in an applied field of 8 T (Fig. 3C, *hatched marks*). The solid line shown in Fig. 3C is a spectrum of the 25-ms sample recorded under identical conditions and scaled to 56% of the total absorption intensity of the spectrum of the 440-ms sample. Removal of this contribution of the Fe^{2+} species from the 440-ms spectrum thus results in a spectrum of $\text{R2}_{\text{peroxo}}$ at 125 K and in 8 T (Fig. 3D, *hatched marks*). Analysis of this spectrum yields an

internal field of 0.95 T, which corresponds to $J = 50 \pm 10$ cm^{-1} . The solid line shown in Fig. 3D is a theoretical simulation using the parameters obtained from the zero-field spectrum (Fig. 3B) and assuming an internal field of 0.95 T. Again, consideration of higher excited states is essential. For example, the $S=3$ and $S=4$ states have Boltzmann population factors of only 5.7% and 0.7%, but contribute 22.0% and 4.7% to $\langle S \rangle_{\text{av}}$, respectively.

Discussion

Mössbauer spectroscopy has been used to determine the exchange coupling constant J of two spectroscopically distinct peroxodiferric reaction intermediates, $\text{R2}_{\text{peroxo}}$ and F_{peroxo} , generated in the reactions of O_2 with the site-directed variant R2-W48F/D84E from *E. coli* and with the M ferritin from frog, respectively. Spectra recorded at 4.2 K show that both $\text{R2}_{\text{peroxo}}$ and F_{peroxo} are antiferromagnetically coupled, resulting in a diamagnetic ground state ($S=0$). At 125 K and in an applied field of 8 T, small internal fields of 0.95 T and 0.60 T, caused by population of excited spin states with $S \geq 1$, are observed for $\text{R2}_{\text{peroxo}}$ and F_{peroxo} , respectively. From the magnitude of the internal field, the exchange coupling constants were determined to be $J = 75 \pm 10$ cm^{-1} for F_{peroxo} and $J = 50 \pm 10$ cm^{-1} for $\text{R2}_{\text{peroxo}}$. Interestingly, the analysis revealed that even though higher excited spin states ($S=2$ and $S=3$) may have negligible populations, they contribute significantly to the spin expectation value and may not be neglected for the determination of J .

Although resonance Raman data [14, 18] indicate a common μ -1,2 binding mode for the peroxide ligand in both $\text{R2}_{\text{peroxo}}$ and F_{peroxo} , on the basis of their distinct spectroscopic properties [6, 12, 14, 17, 18], it is likely that these two reaction intermediates have different core structures. Particularly, EXAFS investigation of F_{peroxo} has revealed a very short Fe-Fe distance of 2.53 Å, suggesting a Fe-O-O angle of 107° [18], while the spectroscopic properties of $\text{R2}_{\text{peroxo}}$ are very similar to those of a structurally known peroxodiferric complex having a Fe-Fe distance of 4.0 Å and a Fe-O-O angle of 129° [15, 25]. The resonance Raman data of F_{peroxo} and $\text{R2}_{\text{peroxo}}$ are consistent with these angular assignments [18, 26]. A detailed computational study on the exchange interaction of μ -1,2-peroxodiferric complexes, carried out by Brunold et al. [26], has concluded that the exchange interaction via the peroxide bridge is rather insensitive to variations in the Fe-O-O angle and Fe-O-O-Fe dihedral angle owing to the numerous exchange pathways that contribute more or less with different cluster geometries. Our observation of similar antiferromagnetic exchange interactions in the two peroxodiferric intermediates, which are likely to have different core structures, supports this conclusion. The short Fe-Fe distance determined for F_{peroxo} requires at least two single atom bridges [19], which may include a μ -1,1 bridging

carboxylate from the protein and/or a bridging hydroxo or aqua ligand. The presence of such ligands is supported by the Fe-O shell at ~ 2.0 Å observed in the EXAFS spectrum of F_{peroxo} [19]. These single-atom bridges provide additional super-exchange pathways and may explain why the J value of F_{peroxo} is 50% larger than that of $R2_{\text{peroxo}}$. The contribution of these pathways can be estimated from diferric compounds having a $\text{Fe}_2(\text{OR})_2$ core, for which the J values range from 20 to 50 cm^{-1} [27, 28, 29, 30, 31]. Thus, the contribution to exchange coupling involving pathways via the peroxide bridge may be very similar in F_{peroxo} and $R2_{\text{peroxo}}$ (i.e., about 50 cm^{-1}). Brunold et al. [26] have also predicted that the exchange interaction of μ -1,2-peroxodiferric complexes is considerably weaker than that of μ -oxodiferric complexes owing to a less covalent Fe-O bond in the peroxo complexes. The moderate exchange interactions determined for these two peroxodiferric intermediates are consistent with this theoretical prediction.

To the best of our knowledge there are only two non-heme peroxodiferric model compounds for which J values have been reported. One compound is the peroxide complex mentioned above with a μ -1,2-peroxide and two μ -1,3-benzoate ligands [15, 25]. Its J value was determined by temperature-dependent magnetization measurements to be 66 cm^{-1} [25], comparable to that of F_{peroxo} and $R2_{\text{peroxo}}$. The other peroxodiferric complex was generated by oxygenation of a μ -alkoxo- μ -1,3-benzoate bridged diferrous compound at low temperatures and was proposed to have a μ -alkoxo- μ -1,2-peroxo- μ -1,3-benzoate- Fe_2 core [32]. The J value of this complex was determined by temperature-dependent ^1H NMR spectroscopy to be $\sim 140 \text{ cm}^{-1}$, which is more than double the values observed for the other three peroxodiferric compounds discussed here. Currently, there is no satisfactory explanation for the large difference in J observed for these two peroxodiferric complex.

In conclusion, we have used Mössbauer spectroscopy to determine the exchange coupling constant J of antiferromagnetically coupled diferric reaction intermediates. The approach makes use of the unique capability of Mössbauer spectroscopy to detect the internal fields at the Fe nuclei of Fe complexes. The magnitude of the internal field depends on (1) the thermal populations of the excited paramagnetic spin states and (2) the population difference of the sub-spin states (states with the same S but different M values) induced by the Zeeman interaction. The former depends on the energy of the excited state, which is a function of J , and the latter depends on the external applied field. For antiferromagnetically coupled diferric systems with weak to moderate coupling constants, internal fields on the order of 1 T can be induced in the temperature range of 100–200 K in an external field of 8 T. These conditions allow a rather accurate determination of J . For strongly antiferromagnetically coupled systems, the energies of the excited states are higher, resulting in lesser populations of the excited states, and thus, smaller internal fields. Larger internal fields, however, can be realized by the

application of a stronger external field to induce a larger population difference for the sub-spin states. For example, for an antiferromagnetically coupled diferric cluster with $J = 150 \text{ cm}^{-1}$, the application of a magnetic field of 12 T at 200 K can generate an internal field of 0.42 T, a value that can be accurately detected by Mössbauer spectroscopy. In principle, this method is also applicable to diiron complexes of other oxidation states or to hetero-binuclear Fe complexes, provided that an appropriate theoretical model exists for describing the electronic properties of the system. The major advantage of this method is that it can be applied to the study of reaction intermediates trapped by the rapid freeze-quench technique, to which the conventional methods used for determination of J , such as the saturation magnetization measurement and ^1H NMR spectroscopy, are not applicable because the presence of other paramagnetic species in the freeze-quenched sample (e.g., the not-yet-reacted Fe^{2+}) would render the magnetization data uninterpretable, and ^1H NMR spectroscopy cannot be applied to frozen samples.

Acknowledgements This work is supported in part by NIH grants GM58778, GM47295 (B.H.H.), GM55365 (J.M.B.), and DK20251 (E.C.T.).

References

1. Wallar BJ, Lipscomb JD (1996) *Chem Rev* 96:2625–2657
2. Feig AL, Lippard SJ (1994) *Chem Rev* 94:759–805
3. Fox BG, Shanklin J, Somerville C, Münck E (1993) *Proc Natl Acad Sci USA* 90:2486–2490
4. Sjöberg B-M (1997) *Struct Bonding* (Berlin) 88:139–173
5. Pereira AS, Tavares P, Lloyd SG, Danger D, Edmondson DE, Theil EC, Huynh BH (1997) *Biochemistry* 36:7917–7927
6. Pereira AS, Small W, Krebs C, Tavares P, Edmondson DE, Theil EC, Huynh BH (1998) *Biochemistry* 37:9871–9876
7. Valentine AM, Stahl SS, Lippard SJ (1999) *J Am Chem Soc* 121:3876–3887
8. Liu KE, Wang D, Huynh BH, Edmondson DE, Salifoglou A, Lippard SJ (1994) *J Am Chem Soc* 116:7465–7466
9. Liu KE, Valentine AM, Wang D, Huynh BH, Edmondson DE, Salifoglou A, Lippard SJ (1995) *J Am Chem Soc* 117:10174–10185
10. Broadwater JA, Ai J, Loehr TM, Sanders-Loehr J, Fox BG (1998) *Biochemistry* 37:14664–14671
11. Broadwater JA, Achim C, Münck E, Fox BG (1999) *Biochemistry* 38:12197–12204
12. Bollinger JM Jr, Krebs C, Vicol A, Chen S, Ley BA, Edmondson DE, Huynh BH (1998) *J Am Chem Soc* 120:1094–1095
13. Baldwin J, Voegtli WC, Khidkel N, Moëne-Loccoz P, Krebs C, Pereira AS, Ley BA, Huynh BH, Loehr TM, Riggs-Gelasco PJ, Rosenzweig AC, Bollinger JM Jr (2001) *J Am Chem Soc* 123:7017–7030
14. Moëne-Loccoz P, Baldwin J, Ley BA, Loehr TM, Bollinger JM Jr (1998) *Biochemistry* 37:14659–14663
15. Kim K, Lippard SJ (1996) *J Am Chem Soc* 118:4914–4915
16. Treffry A, Zhao Z, Quail MA, Guest JR, Harrison PM (1995) *Biochemistry* 34:15204–15213
17. Fetter J, Cohen J, Danger D, Sanders-Loehr J, Theil EC (1997) *J Biol Inorg Chem* 2:652–661
18. Moëne-Loccoz P, Krebs C, Herlihy K, Edmondson DE, Theil EC, Huynh BH, Loehr TM (1999) *Biochemistry* 38:5290–5295
19. Hwang J, Krebs C, Huynh BH, Edmondson DE, Theil EC, Penner-Hahn JE (2000) *Science* 287:122–125

20. Kauffmann KE, Münck E (1998) In: Solomon EI, Hodgson KO (eds) Spectroscopic methods in bioinorganic chemistry. (ACS Symp Ser, vol 692) American Chemical Society, Washington, pp 16–29
21. Zang Y, Dong Y, Que L Jr, Kauffmann KE, Münck E (1995) *J Am Chem Soc* 117:1169–1170
22. Kauffmann KE, Popescu CV, Dong Y, Lipscomb JD, Que L Jr, Münck E (1998) *J Am Chem Soc* 120:8739–8746
23. Bencini A, Gatteschi D (1990) Electron paramagnetic resonance of exchange coupled systems. Springer, Berlin Heidelberg New York
24. Trautwein AX, Bill E, Bominaar EL, Winkler H (1991) *Struct Bonding (Berlin)* 78:1–95
25. Kitajima N, Tamura N, Amagai H, Fukui H, Moro-oka Y, Mizutani Y, Kitagawa T, Mathur R, Heerwegh K, Reed CA, Randall CR, Que L Jr, Tatsumi K (1994) *J Am Chem Soc* 116:9071–9085
26. Brunold TC, Tamura N, Kitajima N, Moro-Oka Y, Solomon EI (1998) *J Am Chem Soc* 120:5674–5690
27. Borer L, Thalken L, Ceccarelli C, Glick M, Zhang JH, Reiff WM (1983) *Inorg Chem* 22:1719–1724
28. Chiari B, Piovesana O, Tarantelli T, Zanazzi PF (1982) *Inorg Chem* 21:2444–2448
29. Ménage S, Que L Jr (1990) *Inorg Chem* 29:4293–4297
30. Thich JA, Ou CC, Powers D, Vasiliou B, Mastropaolo D, Potenza JA, Schugar HJ (1976) *J Am Chem Soc* 98:1425–1433
31. Walker JD, Poli R (1990) *Inorg Chem* 29:756–761
32. Dong Y, Ménage S, Brennan BA, Elgren TE, Jang HG, Pearce LL, Que L Jr (1993) *J Am Chem Soc* 115:1851–1859